Chinese J. Chem. Eng., **13** (2) 218 – 224 (2005)

Dynamic Thermal Model and Temperature Control of Proton Exchange Membrane Fuel Cell Stack

SHAO Qinglong(邵庆龙)*, WEI Dong(卫东), CAO Guangyi(曹广益) and ZHU Xinjian(朱新坚)
Fuel Cell Institute, Shanghai Jiao Tong University, Shanghai 200030, China

Abstract A dynamic thermal transfer model of a proton exchange membrane fuel cell (PEMFC) stack is developed based on energy conservation in order to reach better temperature control of PEMFC stack. Considering its uncertain parameters and disturbance, we propose a robust adaptive controller based on backstepping algorithm of Lyaponov function. Numerical simulations indicate the validity of the proposed controller.
Keywords proton exchange membrane fuel cell stack, dynamic thermal transfer model, temperature control

1 INTRODUCTION

Non-polluting energy conversion and power generation technology is proposed for the environmental problems brought by normal fuels, and proton exchange membrane fuel cell (PEMFC) is a good choice for its non-polluting character. PEMFC is a device for energy conversion with high efficiency. It directly converts chemical energy into electric energy via electrochemical reaction. PEMFC has become a new generation of power technology, which has been developing in many countries.

In the past decades, researchers focused on optimizing PEMFC stacks so as to improve their performance and cost, which is vital to compete with normal energy conversion devices. The thermal management is one of key factors that affect the performance of PEMFC stack, since the temperature within PEMFC stack rises quickly with the heat produced by electrochemical reaction and the heat brought by humid reactant gas. As the temperature goes higher than 100℃, the output performance of the stack will be reduced due to losing water from the membrane and increasing vapor pressure. In particular, excessive thermal stresses may cause rupture of the membrane. On the contrary, excessive low temperature will limit the mass transport in the stack and decrease electrochemical reaction rates. Therefore, it is important to keep the stack thermal balance under given operating temperature (in general 80℃), which ensures better performance of the stack.

For getting a better thermal management of the PEMFC stack, it is necessary to develop the thermal transfer model, and find the suitable control method on the basis of this transfer model. Some authors[1−5] have proposed many thermal models for a single cell, which account for various physical processes, but do not fit for temperature control in stack. However, the thermal model of PEMFC stack is seldom reported. Lee *et al.*[6], carried out work on a stack which was divided into a lot of computational elements and the thermal balance for one of them was analyzed, then the temperature distribution in the stack was obtained by summing all elements according to the boundary conditions. However, the calculations increased with power and model accuracy increased. Amphlett *et al.*[7] developed a thermal transfer transient model of stacks and analyzed the transient temperature variation with load current. However, they did not consider thermal radiation and Ohmic heat. In addition, the literatures on the temperature control of stack are scarce. Lee *et al.*[8], based on the model of Lee *et al.*[6], presented a controlling algorithm of limited amplitude. The temperature in stack was controlled by comparing the operating temperature with the maximum and minimum values of temperature allowed (the values was not given in Ref. [8]). Although this controlling algorithm was simple, the temperature control accuracy may be not high (the controlling results are not given). H. I. Lee *et al.*[9] made use of PID algorithm to control temperature in stack, and the controlling accuracy was low.

For all problems mentioned above, it is necessary to develop a simple model for dynamic thermal transfer, and find suitable control method for it. In this paper, we develop a more perfect dynamic thermal transfer model of PEMFC stack based on the modelling of Amphlett *et al.*[7]. This model will be nonlinear with uncertainties and disturbances as shown later. The main reasons are as follows. (1) There are many physical parameters to be determined by experiments, and every parameter may be different greatly under different conditions. Therefore, they are pro-

Received 2004-03-16, accepted 2004-09-18.
* To whom correspondence should be addressed. E-mail: sql102@sjtu.edu.cn

cessed as uncertainties in this paper. (2) It is difficult to analyze the thermal transfer in a stack due to its complicated construction, so accurate thermal transfer model may not be established. (3) There exists load disturbance (the variation of load current). According to these characteristics and comparing various control algorithms, we propose a robust control algorithm to fit to an inaccurate model with uncertainties and disturbances. At the same time, in order to better control temperature in a stack some uncertain parameters are estimated on line. Thus, the scheme in this paper is a robust adaptive control algorithm.

2 DYNAMIC THERMAL TRANSFER MODEL OF A PEMFC STACK

Before describing the formulation of this model, a brief description of the operation of a PEMFC stack will be given. Diagram of a typical section of the stack is shown in Fig. 1(a). A single cell, which can be described as membrane electrode assemblies (MEA), is composed of a membrane electrolyte sandwiched between two porous electrodes. Bipolar plates (graphite plate), with electrical conduction, separate the MEAs as well as provide a means for delivery of the fuel (H_2) and oxidant (air) to the reaction sites located at the electrode membrane interface. The basic unit is repeated to build up a stack. Considering the difference of stack power, a complete multi-cell stack may include cooling plates, which are specially designed in bipolar plates.

In addition, in order to ensure the uniformity of temperature distribution for a stack, we consider that cooling plates are not collocated uniformly. In the middle part of a stack, the cooling plates are collocated as shown in Fig. 1(b), and on both sides in the stack as illustrated in Fig. 1(c).

2.1 Dynamic thermal transfer of PEMFC stack

In this section, the dynamic thermal transfer model of PEMFC stack is developed according to the energy conservation principle. For simplification, some necessary assumptions are given as follows: (1) All gases are ideal gases and fully saturated with water vapor. (2) The membranes are fully hydrated. (3) The produced water is in the liquid phase. (4) Since the temperature distribution in a stack is not uniform, in the model, the temperature in stack is known as the highest temperature within the single cell in the stack. (5) The flow of cooling water in the stack is laminar.

Under steady state, the stack energy equilibrium is between the input and the heat produced and the heat released. The input and heat produced include the heat brought in by reactant gas, the heat produced by electrochemical reaction and Ohmic heat produced by stack resistance. The releasing heat includes the radiation from the surface of stack, the heat brought out by exhaust gas and water produced, and the convection between stack and cooling water. Considering the transient heat variation, the dynamic thermal model can be described as follows

$$MC\frac{\mathrm{d}T_1}{\mathrm{d}t} = q_{\mathrm{act}} + q_{\mathrm{resis}} + q_{\mathrm{in}} - q_{\mathrm{out}} - q_{\mathrm{conv}} - q_{\mathrm{rad}} \quad (1)$$

where q_{act} denotes the heat produced by electrochemical reaction, q_{resis} denotes Ohmic heat produced by stack resistance, q_{in} the heat brought in by input gas, q_{out} the heat brought out by exhaust gas and produced water, q_{conv} the convection between stack and cooling water, q_{rad} the radiation from the surface of stack, T_1 is the stack temperature, M denotes the stack mass, and C is the average specific heat of stack.

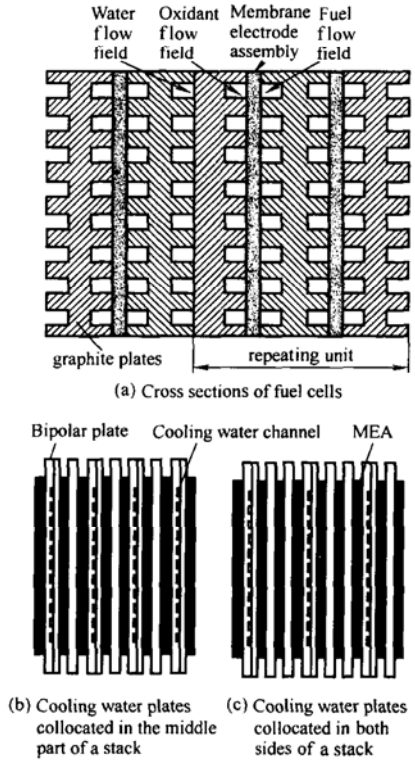

Figure 1 Schematic of a PEM fuel cell satck

2.1.1 *calculation of* q_{act}

The generation of heat is due to entropy change as well as irreversibilities related to the charge transfer in a single cell.

$$q_{\mathrm{act}} = \left[\frac{T_1(-\Delta S)}{nF} + \eta_{\mathrm{act}}\right] AZi \quad (2)$$

where η_{act} can be obtained by the following Butler-Volmer equation

$$i = i_0^{\mathrm{ref}}\left(\frac{c_{\mathrm{O_2}}}{c_{\mathrm{O_2}}^{\mathrm{ref}}}\right)\left[\exp\left(\frac{\alpha_{\mathrm{a}}F}{RT_1}\eta_{\mathrm{act}}\right) - \exp\left(-\frac{\alpha_{\mathrm{c}}F}{RT_1}\eta_{\mathrm{act}}\right)\right] \quad (3)$$

The oxygen concentration in cathode diffusion layer can be expressed as follows[10]

$$c_{O_2} = \frac{p_{O_2}}{RT_1} = \frac{p_0[1+\beta-\beta\exp(\nu i)]}{RT_1} \tag{4}$$

where

$$p_0 = \frac{p_c - p_{sat}}{1+\beta}, \quad \nu = \frac{\psi}{4F\omega}, \quad \psi = \frac{RT_1}{\varepsilon L_d(p_c - p_{sat})}$$

$$\omega = \frac{1}{\tau^2 L_d^2[p_{sat}/(p_c D_{O_2-H_2O}) + (p_c - p_{sat})/(p_c D_{O_2-N_2})]}$$

The heat produced by electrochemical reaction on anode is neglected due to less heat produced.

2.1.2 *Calculation of* q_{resis}

According to Ohmic law, Ohmic heat is calculated as

$$q_{resis} = \frac{i^2}{\kappa} \tag{5}$$

where κ is the resistance coefficient of a stack, and is composed of those of membranes, diffusion layers and bipolar plates. They are determined by experiment and vary with operation conditions.

Let

$$\theta_1 = \frac{1}{\kappa}, \quad \text{then} \quad q_{resis} = \theta_1 i^2 \tag{6}$$

where θ_1 can be estimated on-line, which will be introduced latter.

2.1.3 *Calculation of* q_{in}

The heat brought into a stack by input gas can be described as

$$q_{in} = q_{a,in} + q_{c,in} \tag{7}$$

where

$$q_{a,in} = (m_{in,H_2}C_{H_2} + m_{a,in,H_2O}C_{H_2O})(T_{a,in} - T_1)Z \tag{8}$$

$$q_{c,in} = (m_{in,air}C_{air} + m_{c,in,H_2O}C_{H_2O})(T_{c,in} - T_1)Z \tag{9}$$

$$m_{in,H_2} = \frac{\lambda_{H_2}G_{H_2}A}{2F}i, \quad m_{a,in,H_2O} = \frac{p_{sat}}{p_a - p_{sat}}m_{in,H_2} \tag{10}$$

$$m_{in,air} = \frac{\lambda_{air}G_{air}A}{2F\beta}i, \quad m_{c,in,H_2O} = \frac{p_{sat}}{p_c - p_{sat}}m_{in,air} \tag{11}$$

2.1.4 *Calculation of* q_{out}

In general, the difference in temperature between cathode and anode export is very small, so we consider that the temperatures of the cathode and anode export are equal to the temperature in the stack. Thus the heat brought out by exhaust gas and water produced is calculated by

$$q_{out} = (m_{out,w}C_w + m_{out,H_2}C_{H_2} + m_{out,air}C_{air})(T_1 - T_{sur})Z \tag{12}$$

where

$$\begin{aligned} m_{out,w} &= m_{out,c,w} + m_{out,a,w} \\ &= (\lambda_{H_2} - 1)\frac{iAG_{H_2}}{2F}\frac{p_{sat}}{p_a - p_{sat}} + \left(\frac{\lambda_{air}}{\beta} - 1\right)\cdot \\ &\quad \frac{iAG_{air}}{4F}\frac{p_{sat}}{p_c - p_{sat}} \end{aligned} \tag{13}$$

$$\begin{aligned} m_{out,H_2} &= m_{in,H_2} - \frac{iAG_{H_2}}{2F}, \\ m_{out,air} &= m_{in,air} - \frac{iAG_{air}}{4F} \end{aligned} \tag{14}$$

2.1.5 *Calculation of* q_{rad}

On the basis of thermal radiation principle, the radiation heat of stack is expressed as

$$q_{rad} = \phi A_s \sigma(T_1^4 - T_{sur}^4) \tag{15}$$

2.1.6 *Calculation of* q_{conv}

According to the thermal convection principle[11], the heat exchange surface of stack is assumed to be constant surface temperature. Thus the convection between the stack and cooling water is calculated as

$$q_{conv} = A_p h\left(T_1 - \frac{T_2 + T_{sur}}{2}\right) \tag{16}$$

In actual situation, h is difficult to be determined, so we let $\theta_2 = h$, and θ_2 will be estimated latter.

2.2 Dynamic thermal transfer of cooling water

Similar to the stack thermal model, the dynamic thermal transfer of cooling water is described as

$$M_w C_w \frac{dT_2}{dt} = q_{conv} - q_{cool} \tag{17}$$

The heat brought out by the cooling water is

$$q_{cool} = C_w m_w (T_2 - T_{sur}) \tag{18}$$

Substituting Eqs. (2), (5), (7), (12), (15), (16) into Eq. (1) and substituting Eqs.(16) and Eq. (18) into Eq. (17), we get the following expression for the temperature model of PEMFC stack

$$\begin{cases} \dot{T}_1 = -a_1T_1 - a_2T_1^4 + b_1T_2 + a_3 + c_1\theta_1 + \\ \qquad (c_2 - T_1)\theta_2 + (a_4T_1 + a_5T_1\ln T_1 + a_6)i \\ \dot{T}_2 = -b_1T_2 + (b_2 - b_3T_2)m_w + (T_1 - c_2)\theta_2 \\ y = T_1 \end{cases} \tag{19}$$

where the stack temperature T_1 and the cooling water temperature T_2 are state variables, the cooling water flux m_w is the control input, the stack output current density i is a measurable disturbance, which varies with the load, the stack inter-resistance coefficient θ_1 and heat exchange coefficient θ_2 between the stack and cooling water are unknown constants, $a_1 \sim a_6$, $b_1 \sim b_3$, c_1, and c_2 are constant coefficients.

In particular, if there is no heat exchange in the stack, Eq. (19) reduce to

$$\begin{cases} \dot{T}_1 = -a_1T_1 - a_2T_1^4 + b_1T_2 + a_3 + c_1\theta_1 + \\ \qquad (a_4T_1 + a_5T_1\ln T_1 + a_6)i \\ y = T_1 \end{cases} \tag{20}$$

We find that Eq. (19) is a single-input single-output (SISO) nonlinear system with uncertain parameters (*e.g.* θ_1, θ_2) and disturbance.

3 DESIGN OF THE ROBUST ADAPTIVE CONTROLLER

Recently, the problem of robust adaptive control for uncertain nonlinear systems of different forms has been studied widely[12−15] based on the backstepping method of Lyaponov function, which has been applied in robot and electric power. In this section, a robust adaptive control algorithm (RACA) for Eq. (19) will be developed.

In the RACA, the uncertain parameters (*e.g.* θ_1, θ_2) will be estimated and adjusted on-line so that the output of system converges to the reference output signal within required precision and all closed-loop signals should be bounded.

For a clear description, rewrite Eq. (19) as

$$\begin{cases} \dot{T}_1 = b_1T_2 + f_1 + \boldsymbol{\theta}^{\mathrm{T}}\varphi_1 + \psi i \\ \dot{T}_2 = f_2 + \beta m_{\mathrm{w}} + \boldsymbol{\theta}^{\mathrm{T}}\varphi_2 \\ y = T_1 \end{cases} \tag{21}$$

where

$$f_1 = -a_1T_1 - a_2T_1^4 + a_3,$$

$$\boldsymbol{\varphi}_1 = \begin{bmatrix} c_1 \\ c_2 - T_1 \end{bmatrix},$$

$$\boldsymbol{\theta}^{\mathrm{T}} = [\theta_1 \quad \theta_2],$$

$$f_2 = -b_2T_2,$$

$$\psi = a_4T_1 + a_5T_1\ln T_1 + a_6,$$

$$\beta = b_2 - b_3T_2,$$

$$\boldsymbol{\varphi}_2 = \begin{bmatrix} 0 \\ T_1 - c_2 \end{bmatrix}$$

For design of the controller, we describe it as the following steps

Step1: let

$$\tilde{\boldsymbol{\theta}} = \boldsymbol{\theta} - \hat{\boldsymbol{\theta}}, \quad z_1 = T_1 - y_{\mathrm{r}} = y - y_{\mathrm{r}}$$

where $\hat{\boldsymbol{\theta}}$ denotes the estimated parameter of vector $\boldsymbol{\theta}$, y_{r} denotes the reference signal, and z_1 is the tracking error.

With $z_2 = T_2 - \alpha_1$, V_1 is a positive definite function

$$V_1 = \frac{1}{2}z_1^2 + \frac{1}{2}(\boldsymbol{\theta} - \hat{\boldsymbol{\theta}})^{\mathrm{T}}(\boldsymbol{\theta} - \hat{\boldsymbol{\theta}}) \tag{22}$$

The derivative of V_1 along the trajectory of Eq. (21) is given by

$$\begin{aligned} \dot{V}_1 =& z_1\dot{z}_1 - \tilde{\boldsymbol{\theta}}^{\mathrm{T}}\dot{\hat{\boldsymbol{\theta}}} \\ =& z_1(a_1z_2 + a_1\alpha_1 + f_1 + \hat{\boldsymbol{\theta}}^{\mathrm{T}}\boldsymbol{\varphi}_1 + \psi i - \dot{y}_{\mathrm{r}}) + \\ & \tilde{\boldsymbol{\theta}}^{\mathrm{T}}(z_1\boldsymbol{\varphi}_1 - \dot{\hat{\theta}}) \end{aligned} \tag{23}$$

With

$$\boldsymbol{\tau}_1 = z_1\boldsymbol{\varphi}_1 - l_1\hat{\theta},$$

$$\alpha_1 = \frac{1}{a_1}(-c_1z_1 - f_1 - \hat{\boldsymbol{\theta}}^{\mathrm{T}}\boldsymbol{\varphi}_1 - \psi i + \dot{y}_{\mathrm{r}}) \tag{24}$$

where l_1 and c_1 are known constants, and $\omega_1 = \min\left\{c_1, \quad \frac{l_1}{2}\right\}$, we have

$$\dot{V}_1 \leqslant -2\omega_1V_1 + \frac{l_1}{2}\|\boldsymbol{\theta}\|^2 + a_1z_1z_2 + \tilde{\boldsymbol{\theta}}^{\mathrm{T}}(\boldsymbol{\tau}_1 - \dot{\hat{\boldsymbol{\theta}}}) \tag{25}$$

Sep 2: Define a positive definite function V_2 as

$$V_2 = V_1 + \frac{1}{2}z_2^2$$

then its derivative is

$$\begin{aligned} \dot{V}_2 =& \dot{V}_1 + z_2\dot{z}_2 \leqslant -2\omega_1V_1 + \frac{l_1}{2}\|\boldsymbol{\theta}\|^2 + a_1z_1z_2 + \\ & \tilde{\boldsymbol{\theta}}^{\mathrm{T}}(\tau_1 - \dot{\hat{\boldsymbol{\theta}}}) + z_2\Bigg[\beta m_{\mathrm{w}} + f_2 + \tilde{\boldsymbol{\theta}}^{\mathrm{T}}\left(\boldsymbol{\varphi}_2 - \frac{1}{a_1}\frac{\partial\alpha_1}{\partial T_1}\boldsymbol{\varphi}_1\right) + \\ & \hat{\boldsymbol{\theta}}^{\mathrm{T}}\left(\boldsymbol{\varphi}_2 - \frac{1}{a_1}\frac{\partial\alpha_1}{\partial T_1}\boldsymbol{\varphi}_1\right) - \frac{\partial\alpha_1}{\partial T_1}T_2 - \\ & \frac{1}{a_1}\left(\frac{\partial\alpha_1}{\partial T_1}f_1 + \frac{\partial\alpha_1}{\partial T_1}\psi i + \frac{\partial\alpha_1}{\partial i}\dot{i} + \frac{\partial\alpha_1}{\partial\hat{\boldsymbol{\theta}}}\dot{\hat{\boldsymbol{\theta}}} + \right. \\ & \left.\frac{\partial\alpha_1}{\partial y_{\mathrm{r}}}\dot{y}_{\mathrm{r}} + \frac{\partial\alpha_1}{\partial\dot{y}_{\mathrm{r}}}\ddot{y}_{\mathrm{r}}\right)\Bigg] \end{aligned} \tag{26}$$

Defining

$$\boldsymbol{\tau}_2 = \boldsymbol{\tau}_1 + z_2\left(\boldsymbol{\varphi}_2 - \frac{1}{a_1}\frac{\partial\alpha_1}{\partial T_1}\boldsymbol{\varphi}_1\right) \tag{27}$$

$$\begin{aligned} m_{\mathrm{w}} =& \frac{1}{\beta}\Bigg[-c_2z_2 - a_1z_1 - f_2 - \hat{\boldsymbol{\theta}}^{\mathrm{T}}\left(\boldsymbol{\varphi}_2 - \frac{1}{a_1}\frac{\partial\alpha_1}{\partial T_1}\boldsymbol{\varphi}_1\right) + \\ & \frac{\partial\alpha_1}{\partial T_1}T_2 + \frac{1}{a_1}\left(\frac{\partial\alpha_1}{\partial x_1}f_1 + \frac{\partial\alpha_1}{\partial T_1}\psi i + \frac{\partial\alpha_1}{\partial i}\dot{i} + \right. \\ & \left.\frac{\partial\alpha_1}{\partial y_{\mathrm{r}}}\dot{y}_{\mathrm{r}} + \frac{\partial\alpha_1}{\partial\dot{y}_{\mathrm{r}}}\ddot{y}_{\mathrm{r}} + \frac{\partial\alpha_1}{\partial\hat{\boldsymbol{\theta}}}\boldsymbol{\tau}_2\right)\Bigg] \end{aligned} \tag{28}$$

and setting $\omega_2 = \min\{\omega_1, c_1\}$ and $\frac{l_1}{2}\|\boldsymbol{\theta}\|^2 \leqslant M$, we obtain

$$\begin{aligned} \dot{V}_2 = \dot{V}_1 + z_2\dot{z}_2 \leqslant& -2\omega_2V_2 + \frac{l_1}{2}\|\boldsymbol{\theta}\|^2 + \tilde{\boldsymbol{\theta}}^{\mathrm{T}}(\boldsymbol{\tau}_2 - \dot{\hat{\boldsymbol{\theta}}}) + \\ & \frac{z_2}{a_1}\frac{\partial\alpha_1}{\partial\hat{\boldsymbol{\theta}}}(\boldsymbol{\tau}_2 - \dot{\hat{\boldsymbol{\theta}}}) \end{aligned} \tag{29}$$

Let

$$\dot{\hat{\theta}} = \tau_2,$$

then

$$\dot{V}_2 = \dot{V}_1 + z_2\dot{z}_2 \leqslant -2\omega_2 V_2 + \frac{l_1}{2}\|\boldsymbol{\theta}\|^2 \leqslant -2\omega_2 V_2 + M \tag{30}$$

From Eq. (30), we can obtain

$$V_2 \leqslant \frac{M}{\omega_2} + \left[V_2(0) - \frac{M}{\omega_2}\right] \mathrm{e}^{-\omega_2 t} \tag{31}$$

where $V_2(0)$ denotes the initial value of V_2.

Since M and ω_2 can be chosen arbitrarily, we give $\varepsilon > 0$ and let $M/\omega_2 < \varepsilon^2/2$, then

$$\frac{z_1^2}{2} \leqslant \frac{M}{\omega_2} + \left[V_2(0) - \frac{M}{\omega_2}\right] \mathrm{e}^{-\omega_2 t} < \frac{\varepsilon^2}{2} \quad \forall t > T > 0 \tag{32}$$

Hence $|y - y_r| < \varepsilon$, for $\forall t > T$ and by Eq. (32), $\|\tilde{\boldsymbol{\theta}}\|$, $\|\tilde{p}\|$ and $\|z_i\|(i = 1, 2)$ are bounded such that $\|\hat{\boldsymbol{\theta}}\|$, $\|\tilde{p}\|$ and $\|x\|$ are also bounded.

4 NUMERICAL SIMULATION

4.1 Simulation parameters of the stack

The parameters used in numerical simulation of the stack are shown in Table 1.

Table 1 Stack parameters for numerical simulation

Parameter	Value
stack power, kW	5
inlet gas temperature, T_{in}, ℃	80
stack mass, M, kg	43
stack size(length×width×high), cm	38 × 21 × 21
stack weight specific heat, MC, kJ·K^{-1}	35
snigle-cell number, Z	35
single-cell active area, A, cm^2	232
entropy change of cathode side reaction, ΔS, J·mol^{-1}·K^{-1}	−326.36
fuel side pressure, p_{a}, Pa	1.013×10^5
air side pressure, p_{c}, Pa	3.039×10^5
air stoichiometric flow ratio, λ_{air}	3
fuel stoichiometric flow ratio, $\lambda_{\mathrm{H_2}}$	1.5
inlet nitrogen-oxygen mole ratio, β	3.76
τL_{d}	0.149
$\varepsilon L_{\mathrm{d}}$	0.026
reference current density, i_0^{ref}, A·cm^{-2}	4.4×10^{-7}
reference oxygen concentration, $c_{\mathrm{O_2}}^{\mathrm{ref}}$, mol·cm^{-3}	4.6×10^{-6}
stefan-Boltzmann constant, σ, W·m^{-2}·K^{-4}	5.67×10^{-8}
emissivity, ϕ	0.8
environmental temperature, T_{sur}, ℃	20

The tracking value of stack temperature here is taken as a constant and set to 80℃ (353 K). In practice, the cooling water is supplied to the stack when the stack temperature is over 67℃ (340 K) and the controller works simultaneously. The initial condition of the stack are $T_{10} = 343$ K, $T_{20} = 333$ K, $\theta_{10} = 6$, and $\theta_2 = 2400$.

4.2 Results of simulation

Figures 2 and 3 show the simulation results of the RACA. Fig. 2(a) shows simulative current density. The typical values of simulative current density are determined as 0.2, 0.6 and 0.7 A·cm^{-2}. The reason is that, from the view of present technique, the current density is scarcely over 0.7 A·cm^{-2} when air is used as the oxidant. On the contrary, stacks need not cool, because at very low current density the input heat and produced heat are less than the released heat.

Figure 2(b) shows that the temperature can better track a given temperature reference value. The temperature fluctuations of stack only occur when current density varies suddenly, then the fluctuations attenuate gradually and achieve the controlling accuracy after a short period of time. The accuracy of the stack temperature in steady state is within 0.2℃ under various loads (stack current density).

In the simulation, the data of cooling water flux obtained by the RACA include negative values and the flux curve shows high frequency vibration, so these data are processed by the limited amplitude and filtering algorithm before they are used to control the temperature in stack, that is, replacing negative values with zero, limiting the maximum value according to the scale of flux adjustor and filtering high-frequency signal. Fig. 2(c) shows that the flux varies with current density. In Fig. 2(c), the flux curve is zero at the beginning because the data are negative and the temperature within the stack does not arrive the setting value. Then the cooling water flux increases with stack temperature. When the temperature reaches to the setting value, the fluctuation of cooling water flux appears and keeps for a period of time, then goes gradually to steady state. Fig. 2(c) also shows the cooling water flux increases with current density.

Figure 3(a) shows that the inter resistance coefficient θ_1 increases with current density in steady state. Because the increase of current density results in an increase of water produced by electrochemical reaction, the water also increases in the membrane, diffusion layers and channels. Hence the resistance of membrane and diffusion layers and the contact resistance between channels and diffusion layers decrease, then, according to Eq. (2.6), θ_1 increases.

Figure 3(b) shows that the heat exchange coefficient θ_2 is nearly invariable with the current density in steady state. Because heat exchange coefficient depends on the conditions in the boundary layer of heat exchange, which depend on the surface geometry and the nature of the fluid motion, *etc*, but it does not relate to the current density.

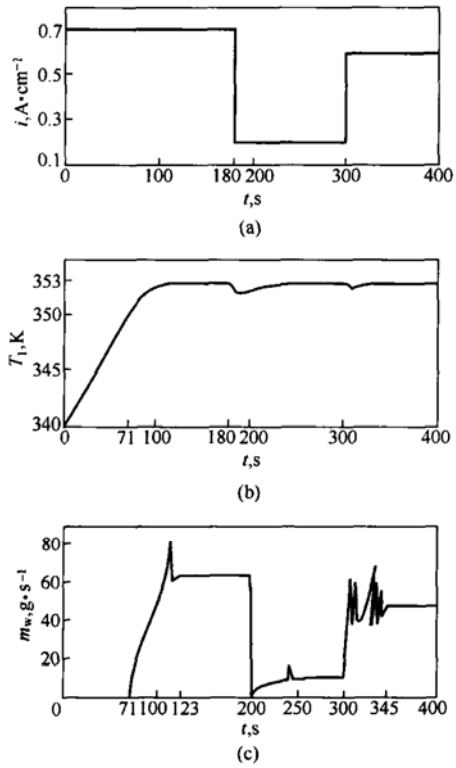

Figure 2 The temperature and the cooling water control curve under different current density based on robust adaptive control algorithm

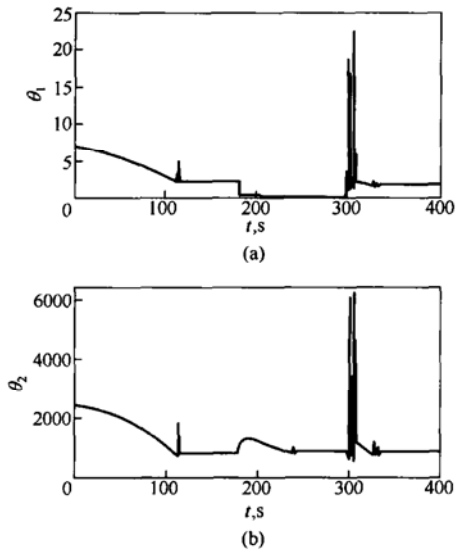

Figure 3 The inter-resistance coefficient and the heat exchange coefficient between the stack and the cooling water with the different current density

In addition, from the results of Figs. 2 and 3, the fluctuations of parameter curve caused by increasing current density are greater than those caused by decreasing current density.

In addition, Lee *et al.* has used PID algorithm to control the temperature in stack for different current densities ($0.2\,A\cdot cm^{-2}$, $0.4\,A\cdot cm^{-2}$, $0.6\,A\cdot cm^{-2}$)[9]. The results are as follows: (1) The temperature value given is 65℃; (2) The minimum error of steady state is zero, the maximum error is 13℃, and the average error is 4℃. By comparing RACA with PID algorithm in literature [9], it is obvious that the controlling accuracy of temperature is higher for RACA. Therefore the RACA is superior to the PID algorithm, and the simulation results show that the RACA is valid for PEMFC temperature control.

5 CONCLUSIONS

In order to better control the temperature of a PEMFC stack, a dynamic thermal transfer model of a PEMFC stack is developed based on the energy conservation of a stack. Since the model is a nonlinear model with uncertain parameters and disturbance, a robust adaptive control algorithm (RACA) is given and a controller is designed based on the backstepping method of Lyaponov function. Numerical simulations show the validity of the proposed controller. By comparing the RACA with the PID, it is shown that RACA is obviously superior to PID for the temperature control of a PEMFC stack. On the other hand, RACA can also be used for other system like Eq. (21).

In future, the dynamic thermal transfer model will be improved further by considering the non-uniformity of temperature distribution. In addition, other parameters (*e.g.* stack specific heat) still are difficult to be determined, and also need to be estimated online. However, the complexity of designing such robust adaptive controller will be increased drastically, and that need further research.

NOMENCLATURE

A	active cell area, cm^2
A_s	surface area of stack, cm^2
C	specific heat, $J\cdot kg^{-1}\cdot K^{-1}$
c	concentration, $mol\cdot cm^{-3}$
D	diffusion coefficient, $cm^2\cdot s^{-1}$
F	Faraday constant, $C\cdot mol^{-1}$
G	molecular weight, $kg\cdot mol^{-1}$
h	heat exchange coefficient, $W\cdot m^{-2}\cdot K^{-1}$
i	current density, $A\cdot cm^{-2}$
L_d	thickness of diffusion layer, cm
M	stack mass, kg
m	mass flux, $kg\cdot s^{-1}$
N	molar flux of diffusion, $mol\cdot cm^{-2}\cdot s^{-1}$
n	number of electrons transferred
p	pressure, Pa
p_0	oxygen partial pressure of channel/diffusion interface, atm
q	heat transfer rate, W
R	universal gas constant, $J\cdot mol^{-1}\cdot K^{-1}$
ΔS	entropy change of cathode side reaction, $J\cdot mol^{-1}\cdot K^{-1}$
T	temperature, K

Z	number of single cell
α	transfer coefficient
β	Inlet nitrogen-oxygen mole ratio
ε	porosity of gas diffusion
η	overpotential, V
λ	stoichiometric flow ratio
σ	Stefan-Boltzmann constant, $W \cdot m^{-2} \cdot K^{-4}$
τ	tortuosity of diffusion layer
ϕ	Emissivity

Superscripts

ref	reference

Subscripts

a	anode
act	activation
air	air
c	cathode
conv	convection
in	input
H_2	hydrogen
H_2O	vapor
N_2	nitrogen
O_2	oxygen
out	output
rad	radiation
resis	resistance
s	surface area
sat	saturation
sur	environment
w	liquid water
1	stack
2, cool	cooling water

REFERENCES

1 Berning, T., Lu, D.M., Djilali, N., "Three-dimensional computational analysis of transport phenomena in a PEM fuel cell", *J. Power Sources*, **106**, 284—294 (2002).

2 Andrew, R., Li, X.G., "Mathematical modeling of proton exchange membrane fuel cells", *J. Power Sources*, **102**, 82—96 (2001).

3 Djilali, N., Lu, D.M., "Influence of heat transfer on gas and water transport in fuel cells", *Int. J. Therm. Sci.*, **41**, 29—40 (2002).

4 Fuller, T.F., Newman, J., "Water and thermal management in solid polymer electrolyte fuel cells", *J. Electrochem. Soc.*, **140**, 1218—1225 (1993).

5 Costamagna, P., "Transport phenomena on polymeric membrane fuel cells", *Chem. Eng. Sci.*, **56**, 323—332 (1993).

6 Lee, J.H., Lalk, T.R., Appleby, A.J., "Modeling electrochemical performance in large scale proton exchange membrane fuel cell stacks", *J. Power Sources*, **70**, 258—268 (1998).

7 Amphlett, J.C., Mann, R.F., Peppley, B.A., Roberge, P.R., Rodrigeus, A., "A model predicting transient responses of proton exchange membrane", *J. Power Sources*, **61**, 183—188 (1996).

8 Lee, J.H., Lalk, T.R., "Modeling fuel cell stack systems", *J. Power Sources*, **73**, 229—241 (1998).

9 Lee, H.I., Lee, C.H., Oh, T.Y., Choi, S.G., Park, I.W., Baek, K.K., "Development of 1 kW class polymer electrolyte membrane fuel cell power generation system", *J. Power Sources*, **107**, 110—119 (2002).

10 Ceraolo, M., Miuli, C., Pozio, A., "Modelling static and dynamic behaviour of pemfc on the basis of electro-chemical description", *J. Power Sources*, **113**, 131—144 (2003).

11 Incropera, F.P., Dewitt, D.P., Fundamentals of Heat Transfer, John Wiley & Sons, New York (1985).

12 Wang, Q.D., Chen, W.T., Chu, X.D., "Robust adaptive control of a class of uncertain nonlinear systems", *Control Theory and Application*, **17**, 244—248 (2000).

13 Ding, Z., "Analysis and design of robust adaptive control for nonlinear output feedback systems under disturbances with unknown bounds", IEEE Proc.-Control Theory Application, **147**, 655—663 (2000).

14 Jiang, Z.P., David, J.H., "A robust adaptive backstepping scheme for nonlinear systems with unmodeled dynamics", IEEE TRANSACTIONS ON AUTOMATIC CONTROL, **44**, 1705—1711 (1999).

15 Huang, C.S., Ruan, R.Y., "Robust adaptive control of a class of uncertain nonlinear systems", Acta Automatica Sinica, **27**, 82—88 (2001).